



Title	Termination of Downward-Oriented Gamma-Ray Glow by Normal-Polarity In-Cloud Discharge Activity
Author(s)	Wada, Y.; Wu, T.; Wang, D. et al.
Citation	Journal of Geophysical Research: Atmospheres. 2023, 128(15), p. e2023JD038606
Version Type	VoR
URL	https://hdl.handle.net/11094/93889
rights	An edited version of this paper was published by AGU. Copyright (2023) American Geophysical Union.
Note	

The University of Osaka Institutional Knowledge Archive : OUKA

<https://ir.library.osaka-u.ac.jp/>

The University of Osaka

JGR Atmospheres

RESEARCH ARTICLE

10.1029/2023JD038606

Key Points:

- A gamma-ray glow was terminated by a lightning flash within a brief time window of 40 ms
- Positive-polarity low-frequency pulses were located within 0.5 km of the detection site
- The glow was ceased by a normal-polarity in-cloud discharge activity between a middle negative layer and an upper positive layer

Correspondence to:

Y. Wada,
wada@yuuki-wd.space

Citation:

Wada, Y., Wu, T., Wang, D., Enoto, T., Nakazawa, K., Morimoto, T., et al. (2023). Termination of downward-oriented gamma-ray glow by normal-polarity in-cloud discharge activity. *Journal of Geophysical Research: Atmospheres*, 128, e2023JD038606. <https://doi.org/10.1029/2023JD038606>

Received 31 JAN 2023

Accepted 20 JUL 2023

Author Contributions:

Conceptualization: Y. Wada
Data curation: Y. Wada, T. Wu, D. Wang, T. Morimoto, Y. Nakamura
Formal analysis: Y. Wada, T. Wu
Funding acquisition: Y. Wada, T. Wu, T. Enoto, H. Tsuchiya
Investigation: Y. Wada, T. Wu, D. Wang, T. Morimoto, Y. Nakamura, T. Shinoda, H. Tsuchiya
Methodology: Y. Wada
Project Administration: Y. Wada
Resources: Y. Wada
Supervision: Y. Wada
Validation: Y. Wada
Visualization: Y. Wada
Writing – original draft: Y. Wada
Writing – review & editing: T. Wu, D. Wang, T. Enoto, K. Nakazawa, T. Morimoto, Y. Nakamura, T. Shinoda, H. Tsuchiya

Termination of Downward-Oriented Gamma-Ray Glow by Normal-Polarity In-Cloud Discharge Activity

Y. Wada¹ , T. Wu² , D. Wang² , T. Enoto^{3,4} , K. Nakazawa⁵ , T. Morimoto⁶ , Y. Nakamura⁷, T. Shinoda⁸, and H. Tsuchiya⁹

¹Division of Electrical, Electronic and Infocommunications Engineering, Graduate School of Engineering, Osaka University, Suita, Osaka, Japan, ²Department of Electrical, Electronic and Computer Engineering, Gifu University, Gifu, Gifu, Japan, ³Department of Physics, Graduate School of Science, Kyoto University, Kyoto, Kyoto, Japan, ⁴Extreme Natural Phenomena RIKEN Hakubi Research Team, Cluster for Pioneering Research, RIKEN, Wako, Saitama, Japan, ⁵Kobayashi-Maskawa Institute for the Origin of Particles and the Universe, Nagoya University, Nagoya, Aichi, Japan, ⁶Faculty of Science and Engineering, Kindai University, Higashiosaka, Osaka, Japan, ⁷Department of Electrical Engineering, Kobe City College of Technology, Kobe, Hyogo, Japan, ⁸Institute for Space-Earth Environmental Research, Nagoya University, Nagoya, Aichi, Japan, ⁹Nuclear Science and Engineering Center, Japan Atomic Energy Agency, Tokai-mura, Ibaraki, Japan

Abstract A gamma-ray glow, a minute-lasting burst of high-energy photons from a thundercloud, was detected by ground-based apparatus at Kanazawa University, Japan, in a winter thunderstorm on 18 December 2018. The gamma-ray glow was quenched by a lightning flash within a brief time window of 40 ms. The lightning flash produced several low-frequency (LF) E-change pulses that were temporally coincident with the termination of the gamma-ray glow, and that were located within 0.5 km from the observation site by the Fast Antenna Lightning Mapping Array. The LF pulses had the same polarity as a positive cloud-to-ground current and a normal-polarity in-cloud current. Since this polarity is against the upward electric field for producing the gamma-ray glow (accelerating electrons to the ground), we infer that the glow was terminated by a normal-polarity in-cloud discharge activity between a middle negative layer and an upper positive layer.

Plain Language Summary Strong electric fields inside thunderclouds may accelerate electrons to relativistic energy, and cause a burst of high-energy photons called gamma-ray glow. Gamma-ray glows are sometimes terminated with a lightning flash as it discharges electric fields responsible for electron acceleration. In this study, we observed the termination of a gamma-ray glow with a detailed lightning mapping observation in the radio-frequency band. An in-cloud lightning flash between two charge layers inside a thundercloud reduced an electric field that accelerated electrons. Radio-frequency observations of glow termination are a powerful tool to investigate the charge structure associated with electron acceleration.

1. Introduction

Gamma-ray glows (also referred to as thunderstorm ground enhancements: TGEs when detected at the ground) are one of the high-energy atmospheric phenomena associated with thunderstorms. They are typically minute-lasting bursts of photons, and their energy spectra extend up to >20 MeV (e.g., Chilingarian et al., 2010; Torii et al., 2002; Tsuchiya et al., 2007). Gamma-ray glows have been detected by aircraft (Kelley et al., 2015; Kochkin et al., 2017, 2021; McCarthy & Parks, 1985; Østgaard et al., 2019; Parks et al., 1981), balloon (Eack & Beasley, 2015; Eack et al., 1996), mountain-top (Bowers et al., 2019; Chilingarian, Mkrtchyan, et al., 2019; Chilingarian et al., 2010, 2022; Chum et al., 2020; Torii et al., 2009; Tsuchiya et al., 2009, 2012), and sea-level experiments (Hisadomi et al., 2021; Kuroda et al., 2016; Torii et al., 2002; Tsuchiya et al., 2007, 2011, 2013; Wada et al., 2018, 2019, 2021a, 2021b). They are thought to originate from bremsstrahlung photons of electrons accelerated and multiplied by strong electric fields inside thunderclouds. There are two candidate mechanisms for electron acceleration. One is the relativistic runaway electron avalanche (RREA: Gurevich et al., 1992). When a thundercloud has an electric field above the RREA threshold (284 kV m⁻¹ at sea-level: Dwyer, 2003), energetic seed electrons can be accelerated by Wilson's runaway electron theory (Wilson, 1925), then can produce secondary electrons. The secondary electrons can be also accelerated, then the number of electrons exponentially increases. With specific conditions, the multiplication mechanism can be boosted by relativistic feedback (Dwyer, 2003, 2012). The other is the modification of the cosmic-ray spectra (MOS: Chilingarian et al., 2012, 2014; Cramer et al., 2017). Even when the strength of an electric field is below the RREA threshold,

charged elementary particles such as electrons, positrons, and muons can gain energy, which causes a slight increase in photon flux. While the MOS regime produces photon-flux increases by a few to a few ten percent from the background, the RREA regime can increase fluxes by several times from the background.

One of the mysteries of gamma-ray glows is where electron acceleration and multiplication occur. In situ measurements of gamma rays and electric fields with airborne equipment are straightforward to identify the position and the strength of electric fields responsible for electron acceleration (Eack & Beasley, 2015; Eack et al., 1996). However, they are limited due to difficulty in cost and opportunity. Instead, multiple-sensory observations such as surface electric field, meteorological radar, and radio-frequency lightning mapping measurements are important to examine the origin of gamma-ray glows (Chilingarian et al., 2017, 2020, 2022; Østgaard et al., 2019; Wada et al., 2018, 2021a). Since gamma-ray glows are produced in thunderclouds, not in lightning discharges, the lightning mapping technique is not applicable to most glows. On the other hand, it can be a powerful tool when a gamma-ray glow is terminated with a lightning discharge.

Wada et al. (2018) previously reported a gamma-ray glow terminated by an intercloud/intracloud discharge with a lightning mapping system in the broadband low-frequency (LF) band. The glow was terminated by a horizontal in-cloud leader progression passing nearby the gamma-ray detector. Kochkin et al. (2018) reported an aircraft observation of a gamma-ray glow termination. The termination was also investigated by the Colorado Lightning Mapping Array, and the lightning location was 12 km ahead of the aircraft. Chilingarian et al. (2017) and Chilingarian, Soghomonyan, et al. (2019) investigated the polarity of in-cloud and cloud-to-ground discharges that terminated TGEs with field-mill measurements (although their method may evaluate the lightning type of irrelevant thundercloud cells to TGEs). On the other hand, the investigation of glow termination with lightning mapping is still limited due to the limited number of glow termination events and dedicated observation campaigns. Here we report another case of glow termination with a broadband LF lightning mapping. The condition of the observation campaign and the detected event is of higher quality than what was reported in Wada et al. (2018).

2. Observation

Winter thunderstorms in the coastal region facing the Sea of Japan are one of the best targets to investigate high-energy atmospheric phenomena. Due to the low-charge-center structure of thunderclouds (Kitagawa & Michimoto, 1994; Michimoto, 1991), high-energy photons are less attenuated in winter thunderstorms than in summer ones before reaching the ground. Therefore, it is possible to detect high-energy atmospheric phenomena at sea level, including gamma-ray glows. In 2016, the Gamma-Ray Observation of Winter Thunderclouds collaboration launched a mapping observation campaign, with multiple gamma-ray detectors distributed in Ishikawa Prefecture, Japan (Yuasa et al., 2020).

Wada et al. (2021b) reported 70 gamma-ray glows from October 2016 to March 2020. Nineteen of the seventy events are categorized to be the lightning-terminated type. Among the lightning-terminated events, one at 14:51:48, 18 December 2018, in the coordinated universal time (UTC), has the second largest count rate at the moment of termination (labeled “Event 50” in Wada et al. (2021b)). This event was detected at Kanazawa University (N36.546°, E136.709°), and also was reported in Wada, et al. (2021a) for radar investigations of glow-producing thunderclouds. The detection was made by our portable-size gamma-ray monitor with a bismuth-germanate crystal of $25.0 \times 8.0 \times 2.5 \text{ cm}^3$ (Yuasa et al., 2020). In the present paper, we focus on this event. Note that another lightning-terminated event at 17:54:50 UTC, 9 January 2018 (labeled “Event 25” in Wada et al. (2021b)) had the largest count rate at the termination, but it is not suitable for the investigation of glow termination because it coincided with a downward terrestrial gamma-ray flash (TGF) (Wada et al., 2019). The exact timing of the glow termination cannot be determined because of the overlap of the downward TGF, a succeeding TGF afterglow by photonuclear reaction, and the glow termination.

The lightning-terminated event on 18 December 2018, was also monitored by the Fast Antenna Lightning Mapping Array (FALMA: Wu et al., 2018, 2020), and by an X-band dual-polarimetric meteorological radar of the Ministry of Land, Infrastructure, Transport and Tourism of Japan. FALMA is an array of flat-plate antennae sensitive to a broadband LF band (0.5–500 kHz) to locate LF pulses from lightning flashes by the time-of-arrival technique. At that time, FALMA consisted of 14 stations and covered around the detection site (Wu et al., 2020). FALMA has the ability to locate LF pulses three-dimensionally, but we utilize only two-dimensional results because the

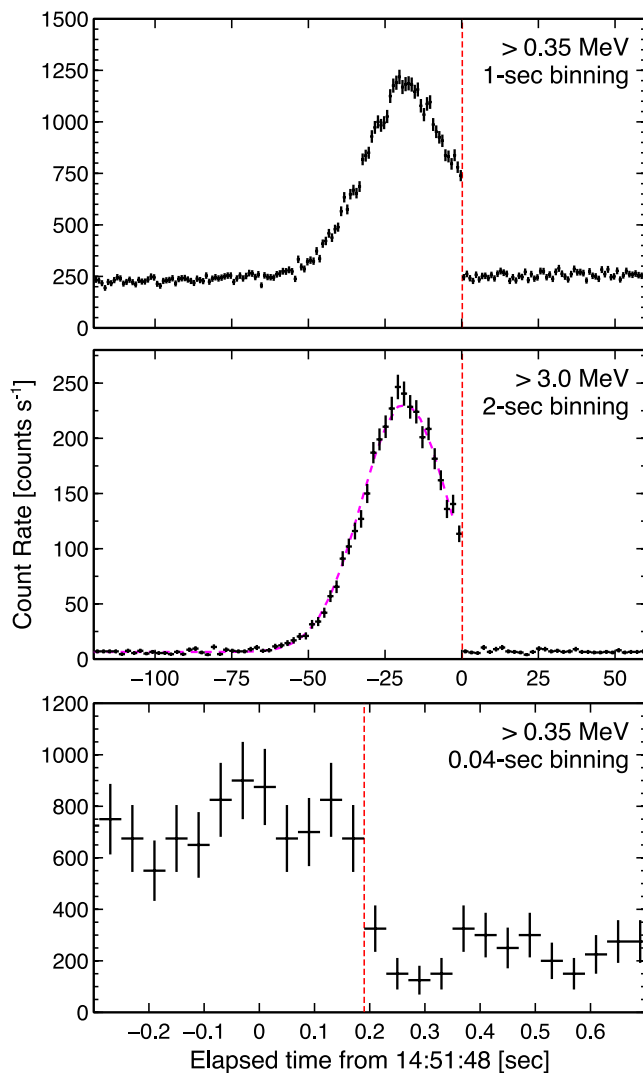


Figure 1. Count-rate histories of the lightning-terminated glow at 14:51:48, 18 December 2018. Upper: Above 0.35 MeV with 1-s binning. Middle: Above 3.0 MeV with 2-s binning. Lower: The expansion around the termination, above 0.35 MeV with 0.04-s binning. The binning origin is set to 190 ms from 14:51:48 UTC, which is shown by the red-dashed lines. The best-fit Gaussian function is overlaid by the magenta-dashed line in the middle panel.

to north-northwest, as in panel (d). The lightning flash initiated 2.9 km northwest of the gamma-ray detector at 171.6 ms from 14:51:48.

The top panel of Figure 3 shows an entire waveform of the lightning flash, recorded by one of the FALMA stations (at N36.894°, E136.779°: 39.16 km from the gamma-ray detector). From the initiation to ~185 ms, there are relatively large in-cloud pulses that are preliminary breakdown (PB) pulses, and following stroke-like pulses. At first, the PB pulses formed an eastward negative leader (NL1 in Figure 2), and then formed a north-eastward negative leader (NL2). After NL1 and NL2, several pulses were located close to the detection site, within the determined time window of the glow termination.

We then extract the LF pulses closely connected to the termination. The criteria are (a) within the time window of the glow termination (14:51:48.170–14:51:48.210) and (b) within 2 km from the gamma-ray detector. These distance criteria are justified as photons in MeV energies are attenuated within ~1 km in the atmosphere at sea level. A total of 6 FALMA-located pulses meet the criteria. Their waveforms and locations are shown in Figure 3.

accuracy of height estimation in winter lightning is relatively low due to the lower charge structure of winter thunderclouds. The X-band radar is located 17.1 km southwest of the detection site. It scans lower elevations every 2 min and higher elevations every 5 min. Therefore, a three-dimensional scan with 12 elevations is obtained every 5 min. Its beam width is 1.2°, and the center frequency is 9.785 GHz. Reflectivity data is attenuation-corrected. At that moment, no field mills were installed beside the gamma-ray detector.

3. Result

Figure 1 shows count-rate histories of the lightning-terminated glow. The energy range of the gamma-ray detector is >0.35 MeV. The energy range above 3 MeV is often used to detect gamma-ray glows with a high signal-to-noise ratio because it is not affected by radon-induced background variations. The count-rate history above 3 MeV can be fitted by a Gaussian function plus a constant offset. The glow has a peak of 18.6 ± 0.2 s before the termination, and the standard deviation of the Gaussian function is 14.1 ± 0.2 s.

We evaluate the exact timing of the termination. The absolute timing of the gamma-ray detector is better than 1 μ s, conditioned by the global positioning system signals. The determination accuracy of the termination timing depends on the photon statistics. In this case, we employ a 40-ms binning to ensure better determination and enough photon statistics for each bin. The 40-ms binned count-rate history is fitted by a step function. One issue is that the origin of binning may affect the fitting result when the transition duration is shorter than the bin width. Therefore, we fit the count-rate history by changing the binning origin. We performed 20 trials by changing the binning origin. The origin is set to be $0.040 \times i/n$ sec from 14:51:48 UTC, where i indicates the i th trial and n is the total number of the trial ($0 \leq i < n$). It means that the binning origin is shifted by 0.002 s every trial. The average termination timing of the 20 trials is 14:51:48.190 with a standard deviation of 0.006 s. Also, the χ^2 fitting error is around 0.006 s. The standard deviation and the fitting error are smaller than half the bin width (0.02 s). Therefore, the termination timing is determined to be $14:51:48.190 \pm 0.020$. In the lower panel of Figure 1, the binning origin is set to 14:51:48.190 UTC. The count rates quickly (less than 40 ms) dropped to the background level.

Figure 2 shows the two-dimensional lightning mapping of the lightning flash at 14:51:48 UTC, obtained by FALMA. The determined glow-termination timing is presented by the magenta areas in panels (b) and (c). The lightning pulses are distributed along a belt-like strong radar echo from south-southeast

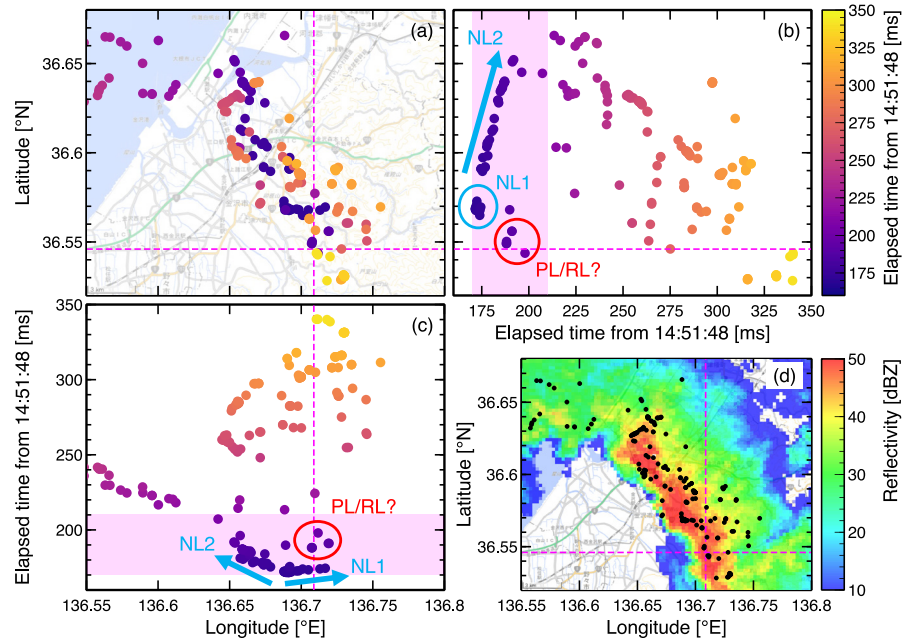


Figure 2. The two-dimensional positions and the time evolution of a lightning flash at 14:51:48 UTC, obtained by Fast Antenna Lightning Mapping Array. (a): Two-dimensional distributions of lightning pulses. The colors of the dots show timing. The magenta-dashed lines indicate the position of the gamma-ray detector. (b) and (c): Timing evolution of the lightning pulses for north-south and west-east directions, respectively. The magenta regions indicate the timing of the glow termination. The blue arrows and circle show negative leaders. The red circles show a possible positive leader and recoil leader. (d) Two-dimensional distributions of lightning pulses on a plan-position-indicator (PPI) image obtained by the X-band radar. The elevation angle of the PPI scan is 3.6°. The background image is provided by the Geospatial Information Authority of Japan.

The waveform of FALMA is recorded in the conventional sign of atmospheric electricity; pulses with positive onsets have the same polarity as a negative cloud-to-ground (CG) current. Pulses 1, 2, 3, and 6 are located within 0.5 km, and Pulses 4 and 5 are ~1.5 km from the gamma-ray detector. Besides the selected pulses, an LF pulse with the largest amplitude in this flash (+18.0 kA) was identified at 189.93 ms, 3.0 km far from the gamma-ray detector.

Figures 4a–4c show vertical cross-sections of multiple plan-position-indicator (PPI) scans by the X-band radar, along the west-east direction. At the moment of the glow detection, the wind blew from west to east with a speed of $11.9 \pm 1.0 \text{ m s}^{-1}$, derived by the pattern-matching technique with low-altitude PPI images (Wada et al., 2021b). A radar echo was found at ~3-km altitude 10 min before the glow detection, and was extending downward 5 min before the detection. At the moment of glow detection, the strong radar echo reached the ground and exhibited a tall and convective structure above the detection site, as previously reported in Wada et al. (2021a). Panel (d) shows the altitudes at 0°C, −10°C, and −20°C, calculated with the mesoscale model (MSM) of the Japan Meteorological Agency. The initial analysis data of MSM at N36.6°, E136.625° and at 15:00 UTC is utilized.

4. Discussion

As mentioned above, the lightning flash had several LF pulses temporally and spatially associated with the glow termination. Pulses 1, 3, and 6 in Figure 3 are located ~0.4 km from the gamma-ray detector. These pulses are the closest to the detector among the selected pulses. On the other hand, we have to consider the movement of the gamma-ray glow as the parent thundercloud moves with the ambient wind flow (Wada et al., 2019; Yuasa et al., 2020). Since the wind speed is estimated to be $11.9 \pm 1.0 \text{ m s}^{-1}$, the wind direction to be eastward, and the peak time of count rates to be $18.6 \pm 0.2 \text{ s}$ before the termination, the center of the glow-emitting region in the thundercloud could be located $221 \pm 19 \text{ m}$ east of the gamma-ray detector. The possible glow center is on the cyan dashed line shown in the lower panel of Figure 3.

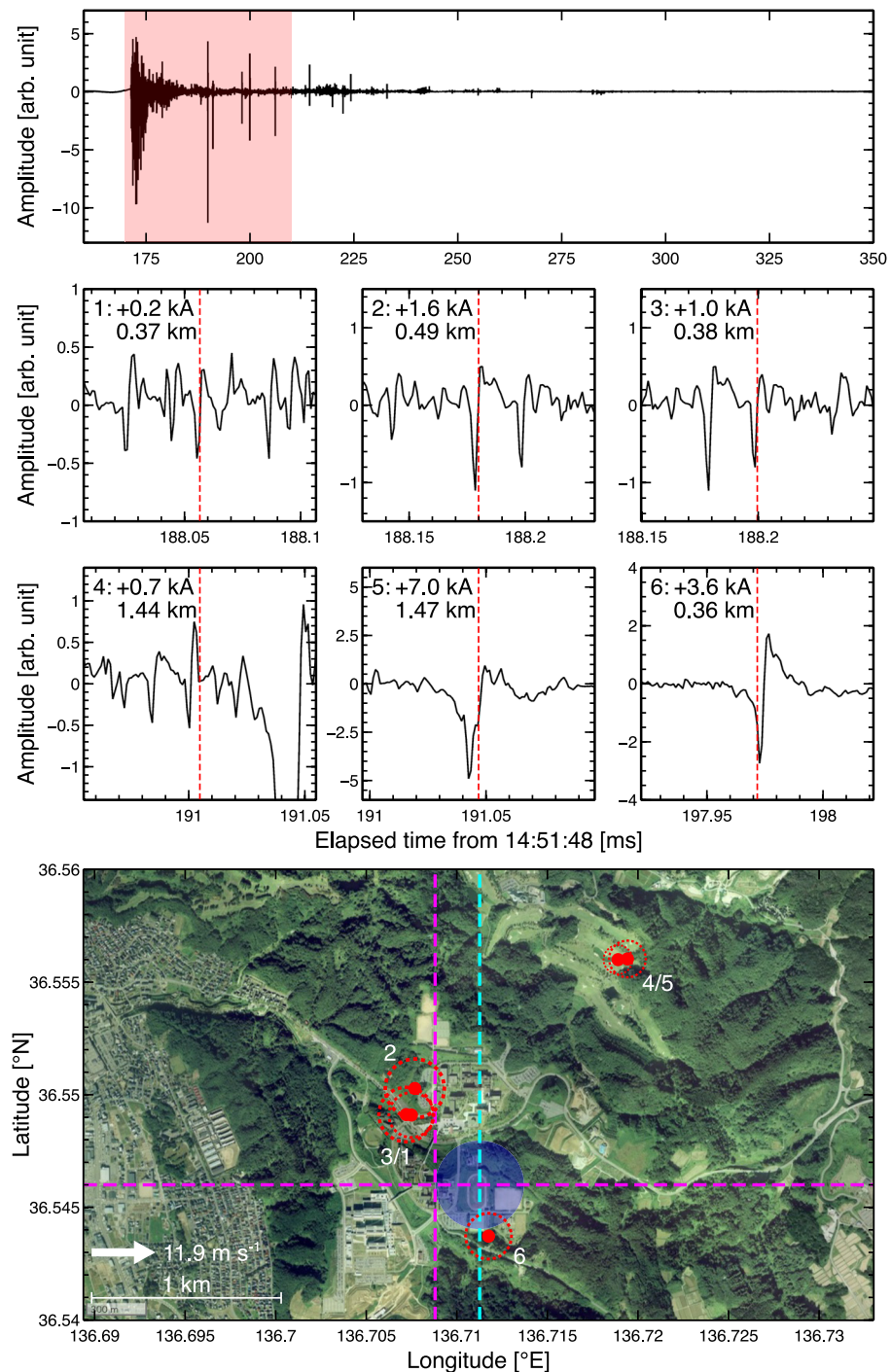


Figure 3. Upper: The entire waveform of the lightning flash, obtained by one of the Fast Antenna Lightning Mapping Array (FALMA) stations. The propagation delay between the antenna and the gamma-ray detector is corrected. The red region shows the determined time window of the glow termination. Middle: Expanded waveforms of the lightning pulses fulfilling the criteria. The red-dashed lines show the detection timing of the pulses by FALMA. The text on the panels shows the peak current and the distance to the gamma-ray detector. Lower: Location of the selected pulses located by FALMA. The red circles indicate the positional estimation error (in root mean square). The magenta-dashed lines indicate the position of the gamma-ray detector. The cyan-dashed line shows a possible position of the glow center at the moment of the glow termination. The blue circle shows an estimated irradiation region of the gamma-ray glow (see the text). The white arrow indicates the wind direction (the wind moved from west to east). The background image is provided by the Geospatial Information Authority of Japan.

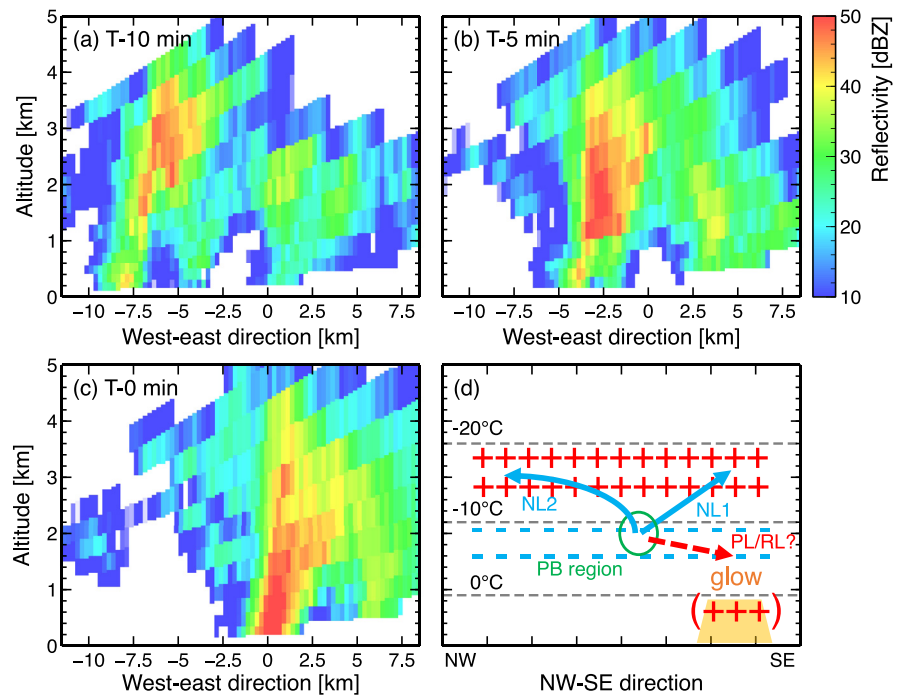


Figure 4. (a), (b), and (c): Vertical cross sections of multiple plan-position-indicator scans by the X-band radar, along the west-east direction. The three panels present 10 and 5 min before the termination and at the moment of the glow termination. The origin of the X-axis is where the gamma-ray detector is installed. The movement of radar echoes by wind flow, due to the difference in scan timing, is corrected. (d): A possible scenario of charge layers and leader progressions inside the thunderclouds. The altitudes of 0°C, -10°C, and -20°C are calculated with the mesoscale model of the Japan Meteorological Agency. Negative leader (NL), positive leader (PL), recoil leader (RL), and preliminary breakdown (PB) stand for NL, PL, RL, and PB, respectively.

The horizontal extension of the glow region should be also considered. In the catalog of gamma-ray glows in winter thunderstorms (Wada et al., 2021b), the duration of gamma-ray glows is defined as T80, the time window containing 80% of the detected photons. When the count-rate history is reproduced by a Gaussian function, T80 (t_{80}) is defined by the integral equation

$$\int_{-\frac{t_{80}}{2}}^{\frac{t_{80}}{2}} \frac{1}{\sqrt{2\pi}\sigma} \exp\left(-\frac{t^2}{2\sigma^2}\right) dt = 0.8, \quad (1)$$

where σ is the standard deviation of the Gaussian function. Since $\sigma = 14.1 \pm 0.2$ s in the present case, T80 is estimated to be 36.1 s. Note that this result is different from the actual T80 reported in Wada et al. (2021b), which includes the effect of the glow termination. The present estimation considers the condition before the glow termination.

Then, the estimated duration is converted to a characteristic width of the gamma-ray glow, 430 m, by multiplying the wind velocity (11.9 m s^{-1}). When the glow center is assumed to be passing right above or closely nearby the detector, we can consider this width as the diameter of the glow region. This assumption is justified as the peak flux of the present case is the third highest among the 70 events in the catalog (Wada et al., 2021b).

By considering the discussion above, we obtain an estimated glow region at the moment of the termination, as shown in the lower panel of Figure 3. This estimated region is closely associated with the electron-acceleration region. The location of Pulse 6 with the estimation error is overlapped with the estimated glow region. Therefore, Pulse 6 is the most plausible candidate for the LF pulse that is directly connected to the glow center.

Pulse 6 has a negative onset, which is the same polarity as positive CGs. Its peak current is estimated to be +3.6 kA. Thus, it is probably a normal-polarity in-cloud (IC) pulse, judged from the small peak current and the

narrow waveform. The second closest pulses such as Pulses 1, 2, and 3 have also a negative onset and small peak current, similar to Pulse 6. Therefore, normal-polarity IC pulses were dominant around the glow region.

Let us consider which charge region was discharged and quenched the gamma-ray glow. To emit gamma rays toward the ground, electrons should be accelerated toward the ground. Therefore, an upward electric field is needed for the gamma-ray glow. So far, several charge structures have been discussed to produce upward electric fields. In the conventional tripole structure (Takahashi, 1978; E. R. Williams, 1989), the electric field between the lower positive and the middle negative layers can accelerate electrons downward. E. Williams et al. (2022) discussed this possibility with surface electric-field and radar observations for TGEs at Mt. Aragats in summer thunderstorms. In the normal dipole structure, similar to the conventional tripole but without the lower positive charge, an upward electric field can be formed between the middle negative layer and the image positive charge layer on the ground. In the inverted charge structure (Saunders & Peck, 1998), the electric field between the lower positive layer and the upper negative layer can do. In fact, Zheng et al. (2019) demonstrated various types of charge structures in winter thunderstorms.

At the beginning of the lightning flash, FALMA detected two NLs, NL1 and NL2 shown in Figure 2. NL1 consists of positive-polarity LF pulses, indicating a negative upward leader progression. The beginning of NL2 consists of positive-polarity LF pulses, and later of mixed-polarity pulses. It indicates that NL2 was at first going upward, and then turned into the horizontal direction. The speed of NL1 and NL2 is almost the same, estimated to be $5.4 \times 10^5 \text{ m s}^{-1}$. Both NL1 and NL2 suggest that the PB happened in a strong negative charge region, then the two leaders were going upward to an upper positive charge layer. Therefore, the entire charge structure of the thundercloud is likely the conventional tripole or the normal dipole structure with the main negative and upper positive layers, not the inverted structure. The schematics are shown in Figure 4d. The gamma-ray glow should have been produced in a strong electric-field region between the main negative charge and the lower positive charge layers (tripole) or between the main negative and the image positive layers (dipole).

How was the strong upward electric field corresponding to the glow depleted? If the upward electric fields are directly discharged, the discharge type should be an inverted polarity IC for the tripole structure, which is the same polarity as a negative CG, or a negative CG stroke for the normal dipole structure. However, the LF pulses associated with the glow termination has the same polarity as a normal-polarity IC. Therefore, the lightning current is likely not to run between the two charge layers forming the upward electric field.

The termination-associated LF pulses occurred immediately after NL1 and NL2. Due to the positive polarity, they possibly originate from a downward positive leader (PL) and a subsequent recoil leader. While FALMA did not capture clearly, it is possible that a positive downward leader was branched from the PB region, going toward the glow-producing region, and finally negative charges above the detection site were depleted, as presented in Figure 4d. In general, positive leaders are less radiative in the LF band than negative ones, and hence hard to detect. On the other hand, a PL could be detected as a recoil leader (RL), when a leader reaches a negative charge region and a lightning current traces the leader channels toward the flash origin (Mazur, 1989; Rakov & Uman, 2003; Rison et al., 1999). When assuming that the PL was initiated simultaneously with the NLs, its speed is estimated to be $1.4 \times 10^5 \text{ m s}^{-1}$, slower than the NLs. Therefore, the most plausible scenario is that the downward PL and the RL in the main negative charge region reduced the upward electric field between the main negative and lower positive layers (tripole), or between the main negative and the image positive layers (dipole). It triggered the glow termination.

We consider not all glows are terminated by such a normal-polarity IC current. For example, Wada et al. (2019) reported a gamma-ray glow terminated with a TGF. While the exact timing of the termination was not determined because the TGF and the following TGF afterglow overlapped, an LF pulse associated with the TGF was located close to the glow center. The LF pulse seems to be a powerful negative return stroke (Wada et al., 2022; Wu et al., 2021) with a peak current of -197 kA , and it is possible that the electric field for the glow production was directly discharged by the negative return stroke.

In conclusion, we presented the termination of a gamma-ray glow by a lightning flash at $190 \pm 20 \text{ ms}$ from 14:51:48 UTC, 18 December 2018, detected at Kanazawa University. The reduction in gamma-ray fluxes was clearly seen in the count-rate history with 40-ms binning, thus the termination was completed within 40 ms. The lightning flash was monitored by the LF network FALMA. The lightning flash consisted of several pulses that were temporally coincident with the termination, and that were also located within 2 km from the detection

site. These pulses were possibly from a downward PL and a RL in the main negative charge layer. Therefore, the upward electric field responsible for downward electron acceleration was reduced by the PL activity in the middle negative layer inside the thundercloud.

Data Availability Statement

The materials presented in this study are available online (Wada, 2023). The XRAIN data set can be obtained through the Data Integration and Analysis System with registration (Data Integration & Analysis System, 2023).

Acknowledgments

The $\text{Be}_2\text{Ge}_3\text{O}_{12}$ scintillation crystal of the present study is provided by Dr. H. Sakurai and Dr. M. Niikura. Dr. T. Sawano, Dr. D. Yonetoku, and Mr. M. Kubo supported the gamma-ray observation at Kanazawa University. The XRAIN data is provided by the Japan Ministry of Land, Infrastructure, Transport and Tourism, retrieved from Data Integration and Analysis System. This research is supported by JSPS/MEXT KAKENHI Grants 16H06006, 19H00683, 21H01116, 21K03681, and 22K14453.

References

- Bowers, G. S., Blaine, W., Shao, X.-M., Dingus, B., Smith, D. M., Schneider, M., et al. (2019). Combining Cherenkov and scintillation detector observations with simulations to deduce the nature of high-energy radiation excesses during thunderstorms. *Physical Review D*, 100(4), 043021. <https://doi.org/10.1103/physrevd.100.043021>
- Chilingarian, A., Daryan, A., Arakelyan, K., Hovhannysyan, A., Mailyan, B., Melkumyan, L., et al. (2010). Ground-based observations of thunderstorm-correlated fluxes of high-energy electrons, gamma rays, and neutrons. *Physical Review D*, 82(4), 043009. <https://doi.org/10.1103/physrevd.82.043009>
- Chilingarian, A., Hovsepian, G., Aslanyan, D., Karapetyan, T., Khanikyan, Y., Kozliner, L., et al. (2022). Thunderstorm ground enhancements: Multivariate analysis of 12 years of observations. *Physical Review D*, 106(8), 082004. <https://doi.org/10.1103/physrevd.106.082004>
- Chilingarian, A., Hovsepian, G., & Vanyan, L. (2014). On the origin of the particle fluxes from the thunderclouds: Energy spectra analysis. *EPL (Europhysics Letters)*, 106(5), 59001. <https://doi.org/10.1209/0295-5075/106/59001>
- Chilingarian, A., Khanikyan, Y., Mareev, E., Pokhsaryan, D., Rakov, V. A., & Soghomonyan, S. (2017). Types of lightning discharges that abruptly terminate enhanced fluxes of energetic radiation and particles observed at ground level. *Journal of Geophysical Research: Atmospheres*, 122(14), 7582–7599. <https://doi.org/10.1002/2017jd026744>
- Chilingarian, A., Khanikyan, Y., Rakov, V., & Soghomonyan, S. (2020). Termination of thunderstorm-related bursts of energetic radiation and particles by inverted intracloud and hybrid lightning discharges. *Atmospheric Research*, 233, 104713. <https://doi.org/10.1016/j.atmosres.2019.104713>
- Chilingarian, A., Mailyan, B., & Vanyan, L. (2012). Recovering of the energy spectra of electrons and gamma rays coming from the thunderclouds. *Atmospheric Research*, 114–115, 1–16. <https://doi.org/10.1016/j.atmosres.2012.05.008>
- Chilingarian, A., Mkrtchyan, H., Karapetyan, G., Chilingaryan, S., Sargsyan, B., & Arestakesyan, A. (2019). Catalog of 2017 thunderstorm ground enhancement (TGE) events observed on Aragats. *Scientific Reports*, 9(1), 6253. <https://doi.org/10.1038/s41598-019-42786-7>
- Chilingarian, A., Soghomonyan, S., Khanikyan, Y., & Pokhsaryan, D. (2019). On the origin of particle fluxes from thunderclouds. *Astroparticle Physics*, 105, 54–62. <https://doi.org/10.1016/j.astropartphys.2018.10.004>
- Chum, J., Langer, R., Baše, J., Kollárik, M., Strhářský, I., Diendorfer, G., & Rusz, J. (2020). Significant enhancements of secondary cosmic rays and electric field at the high mountain peak of Lomnický štít in High Tatras during thunderstorms. *Earth Planets and Space*, 72(1), 28. <https://doi.org/10.1186/s40623-020-01155-9>
- Cramer, E. S., Mailyan, B. G., Celestin, S., & Dwyer, J. R. (2017). A simulation study on the electric field spectral dependence of thunderstorm ground enhancements and gamma ray glows. *Journal of Geophysical Research: Atmospheres*, 122(9), 4763–4772. <https://doi.org/10.1002/2016jd026422>
- Data Integration and Analysis System. (2023). MLIT XRAIN dataset [Dataset]. Retrieved from <https://diasjp.net/service/xrain-data/>
- Dwyer, J. R. (2003). A fundamental limit on electric fields in air. *Geophysical Research Letters*, 30(20), 2055. <https://doi.org/10.1029/2003gl017781>
- Dwyer, J. R. (2012). The relativistic feedback discharge model of terrestrial gamma ray flashes. *Journal of Geophysical Research*, 117(A2), A02308. <https://doi.org/10.1029/2011ja017160>
- Eack, K. B., & Beasley, W. H. (2015). Long-duration X-ray emissions observed in thunderstorms. *Journal of Geophysical Research: Atmospheres*, 120(14), 6887–6897. <https://doi.org/10.1002/2015jd023262>
- Eack, K. B., Beasley, W. H., Rust, W. D., Marshall, T. C., & Stolzenburg, M. (1996). Initial results from simultaneous observation of X-rays and electric fields in a thunderstorm. *Journal of Geophysical Research*, 101(D23), 29637–29640. <https://doi.org/10.1029/96jd01705>
- Gurevich, A., Milikh, G., & Roussel-Dupre, R. (1992). Runaway electron mechanism of air breakdown and preconditioning during a thunderstorm. *Physics Letters A*, 165(5–6), 463–468. [https://doi.org/10.1016/0375-9601\(92\)90348-p](https://doi.org/10.1016/0375-9601(92)90348-p)
- Hisadomi, S., Nakazawa, K., Wada, Y., Tsuji, Y., Enoto, T., Shinoda, T., et al. (2021). Multiple gamma-ray glows and a downward TGF observed from nearby thunderclouds. *Journal of Geophysical Research: Atmospheres*, 126(18), e2021JD034543. <https://doi.org/10.1029/2021jd034543>
- Kelley, N. A., Smith, D. M., Dwyer, J. R., Splitt, M., Lazarus, S., Martinez-McKinney, F., et al. (2015). Relativistic electron avalanches as a thunderstorm discharge competing with lightning. *Nature Communications*, 6(1), 7845. <https://doi.org/10.1038/ncomms8845>
- Kitagawa, N., & Michimoto, K. (1994). Meteorological and electrical aspects of winter thunderclouds. *Journal of Geophysical Research*, 99(D5), 10713. <https://doi.org/10.1029/94jd00288>
- Kochkin, P., Sarria, D., Lehtinen, N., Mezentsev, A., Yang, S., Genov, G., et al. (2021). A rapid gamma-ray glow flux reduction observed from 20 km altitude. *Journal of Geophysical Research: Atmospheres*, 126(9), e2020JD033467. <https://doi.org/10.1029/2020jd033467>
- Kochkin, P., Sarria, D., Skeie, C., van Deursen, A. P. J., de Boer, A. I., Bardet, M., et al. (2018). In-flight observation of positron annihilation by ILDAS. *Journal of Geophysical Research: Atmospheres*, 123, 8074–8090. <https://doi.org/10.1029/2018jd028337>
- Kochkin, P., van Deursen, A. P. J., Marisaldi, M., Ursi, A., de Boer, A. I., Bardet, M., et al. (2017). In-flight observation of gamma ray glows by ILDAS. *Journal of Geophysical Research: Atmospheres*, 122(23), 12801–12811. <https://doi.org/10.1002/2017jd027405>
- Kuroda, Y., Oguri, S., Kato, Y., Nakata, R., Inoue, Y., Ito, C., & Minowa, M. (2016). Observation of gamma ray bursts at ground level under the thunderclouds. *Physics Letters B*, 758, 286–291. <https://doi.org/10.1016/j.physletb.2016.05.029>
- Mazur, V. (1989). Triggered lightning strikes to aircraft and natural intracloud discharges. *Journal of Geophysical Research*, 94(D3), 3311. <https://doi.org/10.1029/jd094id03p03311>
- McCarthy, M., & Parks, G. K. (1985). Further observations of X-rays inside thunderstorms. *Geophysical Research Letters*, 12(6), 393–396. <https://doi.org/10.1029/gl012i006p00393>
- Michimoto, K. (1991). A study of radar echoes and their relation to lightning discharge of thunderclouds in the Hokuriku district. *Journal of the Meteorological Society of Japan. Series II*, 69(3), 327–336. https://doi.org/10.2151/jmsj1965.69.3_327

- Østgaard, N., Christian, H., Grove, J., Sarria, D., Mezentssev, A., Kochkin, P., et al. (2019). Gamma-ray glow observations at 20 km altitude. *Journal of Geophysical Research: Atmospheres*, 124(13), 7236–7254. <https://doi.org/10.1029/2019jd030312>
- Parks, G. K., Mauk, B. H., Spiger, R., & Chin, J. (1981). X-ray enhancements detected during thunderstorm and lightning activities. *Geophysical Research Letters*, 8(11), 1176–1179. <https://doi.org/10.1029/g1008i011p01176>
- Rakov, V. A., & Uman, M. A. (2003). *Lightning: Physics and effects*. Cambridge University Press. Retrieved from <https://books.google.co.jp/books?id=TuMa5IAa3RAC>
- Rison, W., Thomas, R. J., Krehbiel, P. R., Hamlin, T., & Harlin, J. (1999). A GPS-based three-dimensional lightning mapping system: Initial observations in central New Mexico. *Geophysical Research Letters*, 26(23), 3573–3576. <https://doi.org/10.1029/1999gl010856>
- Saunders, C. P. R., & Peck, S. L. (1998). Laboratory studies of the influence of the rime accretion rate on charge transfer during crystal/graupel collisions. *Journal of Geophysical Research*, 103(D12), 13949–13956. <https://doi.org/10.1029/97jd02644>
- Takahashi, T. (1978). Riming electrification as a charge generation mechanism in thunderstorms. *Journal of the Atmospheric Sciences*, 35(8), 1536–1548. [https://doi.org/10.1175/1520-0469\(1978\)035<1536:reaacg>2.0.co;2](https://doi.org/10.1175/1520-0469(1978)035<1536:reaacg>2.0.co;2)
- Torii, T., Sugita, T., Tanabe, S., Kimura, Y., Kamogawa, M., Yajima, K., & Yasuda, H. (2009). Gradual increase of energetic radiation associated with thunderstorm activity at the top of Mt. Fuji. *Geophysical Research Letters*, 36(13), L13804. <https://doi.org/10.1029/2008gl037105>
- Torii, T., Takeishi, M., & Hosono, T. (2002). Observation of gamma-ray dose increase associated with winter thunderstorm and lightning activity. *Journal of Geophysical Research*, 107(D17), ACL2–1–ACL2–13. <https://doi.org/10.1029/2001jd000938>
- Tsuchiya, H., Enoto, T., Iwata, K., Yamada, S., Yuasa, T., Kitaguchi, T., et al. (2013). Hardening and termination of long-duration γ rays detected prior to lightning. *Physical Review Letters*, 111(1), 015001. <https://doi.org/10.1103/physrevlett.111.015001>
- Tsuchiya, H., Enoto, T., Torii, T., Nakazawa, K., Yuasa, T., Torii, S., et al. (2009). Observation of an energetic radiation burst from mountain-top thunderclouds. *Physical Review Letters*, 102(25), 255003. <https://doi.org/10.1103/physrevlett.102.255003>
- Tsuchiya, H., Enoto, T., Yamada, S., Yuasa, T., Kawaharada, M., Kitaguchi, T., et al. (2007). Detection of high-energy gamma rays from winter thunderclouds. *Physical Review Letters*, 99(16), 165002. <https://doi.org/10.1103/physrevlett.99.165002>
- Tsuchiya, H., Enoto, T., Yamada, S., Yuasa, T., Nakazawa, K., Kitaguchi, T., et al. (2011). Long-duration γ ray emissions from 2007 and 2008 winter thunderstorms. *Journal of Geophysical Research*, 116(D9), D09113. <https://doi.org/10.1029/2010jd015161>
- Tsuchiya, H., Hibino, K., Kawata, K., Hotta, N., Tateyama, N., Ohnishi, M., et al. (2012). Observation of thundercloud-related gamma rays and neutrons in Tibet. *Physical Review D*, 85(9), 092006. <https://doi.org/10.1103/physrevd.85.092006>
- Wada, Y. (2023). Materials for “indirect discharge of electric field responsible for gamma-ray glow production” [Dataset]. Mendeley. <https://doi.org/10.17632/H3HTV4RSVJ.2>
- Wada, Y., Bowers, G. S., Enoto, T., Kamogawa, M., Nakamura, Y., Morimoto, T., et al. (2018). Termination of electron acceleration in thundercloud by intracloud/intercloud discharge. *Geophysical Research Letters*, 45(11), 5700–5707. <https://doi.org/10.1029/2018gl077784>
- Wada, Y., Enoto, T., Kubo, M., Nakazawa, K., Shinoda, T., Yonetoku, D., et al. (2021a). Meteorological aspects of gamma-ray glows in winter thunderstorms. *Geophysical Research Letters*, 48(7), e2020GL091910. <https://doi.org/10.1029/2020gl091910>
- Wada, Y., Enoto, T., Nakamura, Y., Furuta, Y., Yuasa, T., Nakazawa, K., et al. (2019). Gamma-ray glow preceding downward terrestrial gamma-ray flash. *Communications Physics*, 2(1), 67. <https://doi.org/10.1038/s42005-019-0168-y>
- Wada, Y., Matsumoto, T., Enoto, T., Nakazawa, K., Yuasa, T., Furuta, Y., et al. (2021b). Catalog of gamma-ray glows during four winter seasons in Japan. *Physical Review Research*, 3(4), 043117. <https://doi.org/10.1103/physrevresearch.3.043117>
- Wada, Y., Morimoto, T., Nakamura, Y., Wu, T., Enoto, T., Nakazawa, K., et al. (2022). Characteristics of low-frequency pulses associated with downward terrestrial gamma-ray flashes. *Geophysical Research Letters*, 49(5), e2021GL097348. <https://doi.org/10.1029/2021gl097348>
- Williams, E., Mkrtchyan, H., Mailyan, B., Karapetyan, G., & Hovakimyan, S. (2022). Radar diagnosis of the thundercloud electron accelerator. *Journal of Geophysical Research: Atmospheres*, 127(11), e2021JD035957. <https://doi.org/10.1029/2021jd035957>
- Williams, E. R. (1989). The tripole structure of thunderstorms. *Journal of Geophysical Research*, 94(D11), 13151. <https://doi.org/10.1029/jd094id11p13151>
- Wilson, C. T. R. (1925). The acceleration of β -particles in strong electric fields such as those of thunderclouds. *Mathematical Proceedings of the Cambridge Philosophical Society*, 22(04), 534–538. <https://doi.org/10.1017/s0305004100003236>
- Wu, T., Wang, D., & Takagi, N. (2018). Lightning mapping with an array of fast antennas. *Geophysical Research Letters*, 45(8), 3698–3705. <https://doi.org/10.1002/2018gl077628>
- Wu, T., Wang, D., & Takagi, N. (2020). Multiple-stroke positive cloud-to-ground lightning observed by the FALMA in winter thunderstorms in Japan. *Journal of Geophysical Research: Atmospheres*, 125(20), e2020JD033039. <https://doi.org/10.1029/2020jd033039>
- Wu, T., Wang, D., & Takagi, N. (2021). Compact lightning strokes in winter thunderstorms. *Journal of Geophysical Research: Atmospheres*, 126(15), e2021JD034932. <https://doi.org/10.1029/2021jd034932>
- Yuasa, T., Wada, Y., Enoto, T., Furuta, Y., Tsuchiya, H., Hisadomi, S., et al. (2020). Thundercloud project: Exploring high-energy phenomena in thundercloud and lightning. In *Progress of theoretical and experimental physics*. <https://doi.org/10.1093/ptep/ptaa115>
- Zheng, D., Wang, D., Zhang, Y., Wu, T., & Takagi, N. (2019). Charge regions indicated by LMA lightning flashes in Hokuriku’s winter thunderstorms. *Journal of Geophysical Research: Atmospheres*, 24, 7179–7206. <https://doi.org/10.1029/2018jd030060>